WOOD RESEARCH
62 (4): 2017
575-586

RESEARCH ON WITHDRAWAL STRENGTH OF MORTISE AND TENON JOINT BY NUMERICAL AND ANALYTIC METHODS

Wen-Gang Hu, Hui-Yuan Guan
Nanjing Forestry University, College of Furnishings and Industrial Design
Nanjing, China

(Received December 2016)

ABSTRACT

In this study, the withdrawal strength of T-shaped joint was investigated through using Finite Element Method (FEM) and Analytic Method (AM). Firstly, the mechanical properties of wood were measured by conducting the experiment. In addition, the influence of friction coefficient between wood interfaces was studied with various size of contact area, direction of grain and pressure. Then, a mathematical model of oval mortise and tenon joint withdrawal strength was established based on linear elastic mechanics. Subsequently, the withdrawal strength of T-shaped joint was analyzed on the basis of numerical method with Finite Element Method (FEM) software. Finally, with the application of the experimental method, comparison and analysis were made between numerical method and analytic method. The results demonstrated that the consistency level between the numerical method and experiment was 83 %, which is more accurate than that between analytic method and experiment 80 %. As a results, the mathematical model was applicable to calculate the withdrawal strength of mortise and tenon joint which can also meet the engineering requirements of wood construction and wooden products structure design. In addition, the FEM applied in the study was more precise than analytic method while the latter was comparatively simple and convenient. These two methods were capable of evaluating the withdrawal strength of mortise and tenon joint, which can also be applied to structure design and optimization of wood construction and wooden products in order to make the design more scientific and reasonable.

KEYWORDS: Mortise and tenon joint, numerical methods, mathematical model, structure design.

INTRODUCTION

As a traditional joint connecting the wooden members, mortise and tenon joints have been widely used in solid wood furniture as well as other wood-frame constructions. Oval and tangential tenon refer to two kinds of common types, which had been extensively investigated in factors influencing the strength of joints, such as scales of mortise and tenon, shape of tenon, adhesive quantity and choice of fit between tenon sides and mortise walls applied in construction of joints, (Smardzewski 2002, Kasal et al. 2015). Admittedly, although the strength of component was enough to carry the load that furniture bear, joint failure had the capability to lead to reducing the strength of the whole structure of furniture. Therefore, it is significantly important to make safe scientific designs of the joints for each component (Smardzewski 2002, 2015b). Even though a universally accepted design formula that calculating the joint strength has not been developed, some useful studies concerning it have still been conducted.

For a long time, Finite Element Methods (FEM) has been being popular among scholars with its widely application in engineering. However, the application in analyzing the mechanical behavior of solid wood mortise and tenon was quite few. Generally speaking, following problems were existed. Firstly, about the material mechanical properties, some studies (Kaygin et al. 2016, Yorur and Uysal 2016) took the wood as isotropic material, which was not able to reflect the anisotropic of wood as generally known. Secondly, other researches (Gavronski 2006, Çolakoglu et al. 2012) considered this point, while taking the joint as rigid, which was not consistent with mortise and tenon joint. Thirdly, although remain studies covered the points above, a reasonable Finite Element Model has not been estublished. Many models (Smardzewski 2004, Prekrat 2010, Kasal et al. 2016) were established based on some hypothesis that the mortise and tenon was clearance fit and the gap was 0.1 mm, which was not consistent with production practice.

The problems mainly concentrated on the joint properties including the selection of fit and the glue-line, However, few studies had been done to determine them. Džinčić and Skakic (2012) investigated the influence of fit on the oval mortise and tenon joint, and found that the strain between mortise and tenon was elastic strain. Furthermore, Džinčić and Živanić (2014) studied the influence of fit on the distribution of glue in oval mortis and tenon joint, the results suggested that for all samples with the gap, the average thickness of the glue layer in the gap amounted to 0.095 mm, and glued line was not interrupted along entire length of joint. By contrast, in joint with overlap fit there is no presence of pure glue.

This study did not solve all problems mentioned above, while focused on the withdrawal force of mortise and tenon based on the friction properties between them. The numerical method and analytic method were used to analyze the withdrawal strength of the joint with interference fit. At first, the mechanical properties of material were measured through carrying out experiment with the corresponding standard, and the friction coefficient of contact surfaces was also studied. Then, a mathematical model of analyzing the strength of joint was established under the hypothesis of linear elastic mechanics. In addition, the numerical method was applied to analyze the strength of mortise and tenon joint. Finally, an experiment was conducted with T-shaped specimens, and the results of the mathematical method and the numerical methods were compared with the experiment. It can be concluded that the numerical and the analytic methods were able to calculate the withdrawal strength of mortise and tenon joint, which can also be applied to design wood structure furniture as well as other wood construction. Withdrawal strength of mortise and tenon joint imposed a significant role in the whole strength of furniture, so it would become more effective in furniture structure design if the withdrawal force was predicted.

MATERIAL AND METHODS

Test materials

All of specimens were made with beech (*Zelkovaserrata* (*Thunb.*) Makino), bought from local commercial supplier. All physical and mechanical parameters of the wood were measured by carefully conducting experiment in accordance with ASTM D 4442 (2001) and ASTM D 143-94(2000), respectively. The average density was 0.69 $g \cdot cm^{-3}$, and the moisture content of wood was conditioned to and held at 12 % before and during experiment.

Description of specimens

The sizes of specimens measuring the mechanical properties of beech and positions pasted the gauge were shown in Fig. 1. Specimen (a) was used to test EL, VLR and VLT, specimen (b) was applied to measure ER and VRT, ET and GRT were measured based on specimen (c) and specimen (d) respectively.

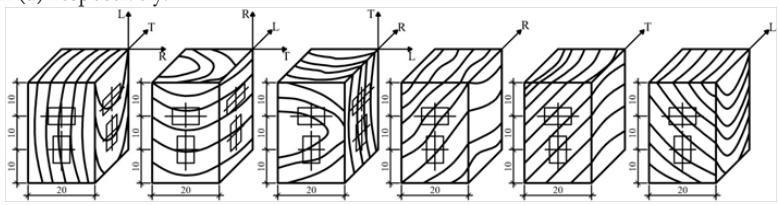

Fig. 1: Specimens measuring mechanical properties of beech.

The specimens measuring the friction coefficient were presented in Fig. 2. With different grain directions, six pairs of contact surfaces were considered, and the sizes of specimen 1 varied from 25 x 25 mm, 25 x 35 mm to 35 x 35 mm respectively with the sizes of specimen 2 being 70 x 35 x 18 mm invariably. Special attention must be paid to the grains and processing path of contact surfaces, which should be consistent with that of mortise and tenon. Besides, the processing path of contact pair R1 was presented in Fig. 3, and other contact pairs were similar to it.

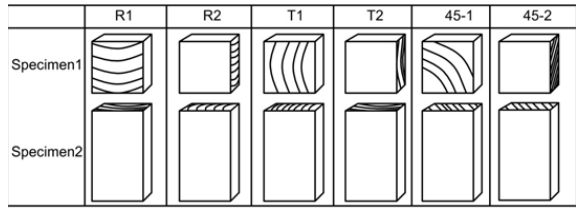

Fig.2: The specimens of different contact pairs.

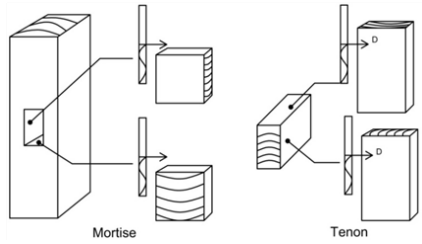

Fig.3: The processing path (b) of specimen.

The T-shaped specimens were constructed of oval mortise and tenon and its detailed size was shown in Fig. 4. Besides, the grain direction of leg and rail cross section were all radical, and the curved surfaces of oval mortise and tenon was 0.12 mm interference fit and flat surfaces were 0.2 mm clearance fit respectively.

All the above specimens were machined by WPC Computer Numerical Control (CNC) machine of Yuan Li with the accuracy of 0.01 mm (Shanghai, China), and the scale of them was measured based on vernier caliper.

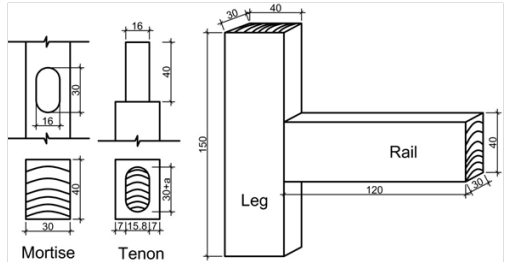

Fig. 4: Size of T-shaped specimen and joint.

Test methods

Through using TDS-530 static data acquisition instrument (TML, Japan), the elastic constants of beech (*Zelkovaserrata* (Thunb.)Makino) were measured, which possessed high accuracy and stability in fast sampling. The elastic modulus and Poisson ratio was tested by conducting compression test, and shear modulus were measured with three points bending test with different spans (Divos et al. 1998).

The friction coefficient of mortise and tenon was measured based on Coulomb Friction Theory with the equipment , as shown in Fig. 5. The loading interface was connected with the universal testing machine, and the force was transformed from vertical to horizontal through the pulley and steel wire which was tied to specimens 1, and then it moved on specimen 2. In addition, the formula of calculating the friction coefficient is like Eq. 1, and each level of every group was tested for 10 times, and the average can be obtained.

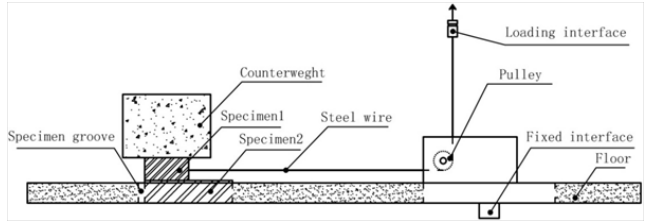

Fig. 5: Equipment of measuring friction coefficient between mortise and tenon.

$$\mu = \frac{F * p}{(m_1 + m_2)g} \tag{1}$$

where: F - maximum force measured by machine,
p - efficiency of the pulley,
m_1, m_2- weight of specimen 1 and specimen 2 respectively,
g - acceleration of gravity.

Withdrawal force of joints were conducted on a 20 KN capacity universal testing machine (SHIMADZU 2012, Japan) at a rate of 10 mm·min^{-1} under static loading.

The test was repeated 20 times, and the schematic diagram of the test was presented in Fig. 6.

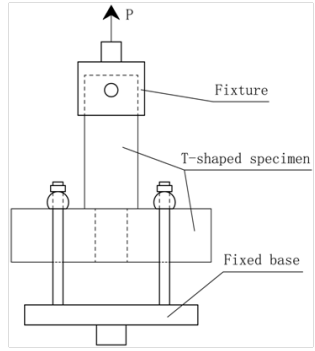

Fig. 6: Schematic diagram of Pull-out test.

RESULTS AND DISCUSSION

Results of experiment

In this study, elasticity and plasticity of material and friction coefficient between mortise and tenon were taken into consideration. Tab. 1 showed the mechanical properties of beech applied in the FEM.

Tab. 1: Mechanical roperties of materials used in joints.

Mechanical properties	**Elastic modulus (N·mm^{-2})**			**Poisson ratio**			**Tangential modulus (N·mm^{-2})**		
	E_L	E_R	E_T	V_{LR}	V_{LT}	V_{RT}	G_{LR}	G_{LT}	G_{RT}
	12567	1374	579	0.450	0.554	0.841	899	595	195
Yield strength	Longitudinal (N·mm^{-2})			Radial (N·mm^{-2})			Tangential (N·mm^{-2})		
	42.51			9.83			4.49		

The results of friction coefficient in different grains, pressure and contact area are provided in Figs. 7a and 7b. According to the results, it can be found that these three factors made no remarkable difference in friction coefficient. Therefore, it can be concluded that friction coefficient of mortise and tenon is a constant (0.54) based on the processing type used in this study. In addition, the results of experiment conformed well with Coulomb friction coefficient, and other studies (Desplanques 2015) also proved this point. However, the friction coefficient of wood-to-wood was quite little and most of them investigated the friction coefficient of steel-to-steel, wood-to-steel and wood-to-rubber and so on (Hüyük et al. 2014, Peng et al. 2012, Shen 2015).

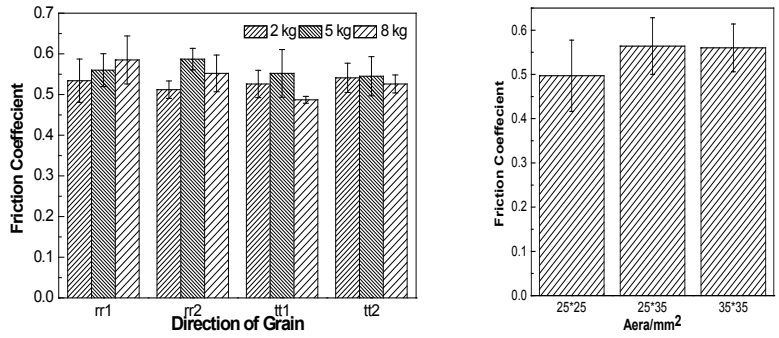

(a) (b)

Fig. 7: Friction coefficient in different load and grain direction(a) and friction coefficient in different contact area(b).

The withdrawal force was measured through using universal testing machine such as Fig. 4. Every specimen was measured by vernier caliper before assembly to guarantee the same interference fit. The results were presented in Fig. 8 and the average of 20 tests was 3192.45 N, and standard error was 398 N.

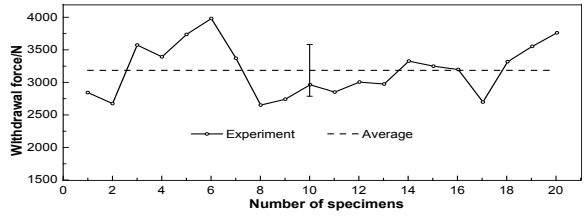

Fig. 8: Results of withdrawal force experiment.

Analytic method

The contact surfaces of oval mortise and tenon joint are curved surfaces which can lead to different strains in different parts of the joint when assembled, so the distribution of stress is not uniform in the joint. With the aim to establish a mathematical model to interpret the distribution of stress in oval mortise and joint, some assumptions below were made in the investigation.

1) The deformation of mortise and tenon joint was elastic strains (Džinčić and Skakic 2012).
2) The curved surfaces of mortise and tenon are completing contact from the macroscopic scale.
3) Stress distribution on any section of joint is same along with the length of the joint.

Then the distribution of stress on curved surfaces will be obtained, if the stress distribution of the arc section was known. The function of stress distribution of curved surface was constructed based on 1/2 arc section due to symmetry, which was just like the shaded part as shown in Fig. 9. Before assembly, every point on the arc section was expressed as Eq. 2. Besides, after assembly, the tenon would be deformed into oval and the corresponding equation was presented in Eq. 3. The interference fit amount between mortise and tenon was defined as $2\Delta b$, and ε_0 was

the maximum strain of vertex on the curved surface of oval tenon, which was calculated by Eqs. 4 and 5. Then, the strains of points on the arc section of tenon could be derived as expression Eq. 6. Furthermore, the stress distribution function of arc section on oval tenon which could be depicted as Eq. 8 based on the Eq. 7.

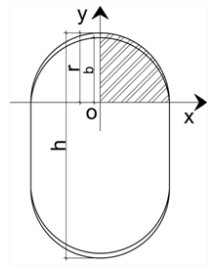

Fig. 9: Schematic diagram of mathematical model.

$$x^2 + y^2 = r^2 \quad (x > 0, y > 0) \tag{2}$$
$$\frac{x^2}{r^2} + \frac{y^2}{b^2} = 1 \quad (x > 0, y > 0) \tag{3}$$
$$\varepsilon_{(0)} = 2\Delta b/h \tag{4}$$
$$\Delta b = r - b \tag{5}$$
$$\varepsilon_{(x)} = \frac{\varepsilon_{(0)}}{b}\sqrt{b^2(1 - x^2/r^2)}\,(0 < x < r) \tag{6}$$
$$\sigma = E \cdot \varepsilon \tag{7}$$
$$\sigma_{(x)} = E \cdot \varepsilon_{(x)} = \frac{2E(r-b)\sqrt{b^2(1-x^2/r^2)}}{hb}\,(0 < x < r) \tag{8}$$

Double integration of a quarter surface of tenon was set up, then the contact force of it was able to obtain shown as Eq. 9 and its simplified Eq. 10. Based on the symmetry, the total contact force of tenon could be worked out as Eq. 11. According to the Coulomb Law of Friction, the frictional force could be expressed as Eq. 12, furthermore, the withdrawal force of joint shown as Eq. 13 was equal to the frictional force based on the Newton's third law.

$$\mathrm{N_{nomal}} = \int_0^{\mathrm{L}} \int_0^{\mathrm{r}} \frac{2E(r-b)\sqrt{b^2(1-x^2/r^2)}}{hb}\, d_x d_L \tag{9}$$
$$N_{nomal} = \frac{\pi ELr\Delta b}{2h} \tag{10}$$
$$N_z = \frac{2\pi ELr\Delta b}{h} \tag{11}$$
$$f = \mu N \tag{12}$$
$$F = \frac{2\mu\pi ELr\Delta b}{h} \tag{13}$$

where: r- radius of arc section of oval tenon , which is also the half thickness of the tenon;
$\varepsilon_{(0)}$- strain of the vertex of arc section;
Δb - half of the interference between mortise and tenon;
b - semi major axis of the ellipse;
N_{nomal}- contact force of oval tenon,
L - length of oval tenon;
f - half friction force of joint;
F - withdrawal force of joint.

Calculated by the mathematical model Eq. 13, the withdrawal force could be obtained as 2928.08N. It needs to be noticed that the wide direction of tenon was radial grain, so when calculation with the mathematical model, elastic modulus ER was supposed to be brought into

the Eq. 13. In addition, the result of analytic method was in a standard deviation compared with that of experiment average, which could satisfy the requirement of engineering design. However, most studies on withdrawal force were nailed and screwed joined based on experimental methods (Douglas et al. 2014, Ringhofer et al. 2014). In addition, the formula calculating the withdrawal force was regressed by experiment data without mechanical theory supporting (Percin 2016).

Numerical analysis

Simulation of stress distribution on the joint of mortise and tenon with interference fit were investigated through using FEM software (Abaqus CAE 6.14-1) in this study. Finite element models were constructed according to the Fig. 2. Then, loads and constraints were applied in accordance to the Fig. 4. In the joint of mortise and tenon, interference fit was imposed to curved surfaces of tenon, and the flat surfaces of tenon were clearance fit. Besides, friction coefficient was obtained by experiment through the method described above, and a displacement load was imposed to the reference point of rail to make the tenon separate from mortise at a constant rate. It is worth of nothing that the wide direction of the tenon was radial. Consequently, the orientation of material properties in FEM must be the same with it, and the withdrawal strength of wood dowel was significantly influenced by ring angle (Wang et al. 2014) Fig. 10 showed the changes of stress distribution in the process of tenon being pulled out. Among them, the Fig 10a was the condition that mortise and tenon were just assembled with interference fit and no load was imposed to rail. Subsequently, with the increase of load, the stress of the constrained parts grew gradually as presented in Fig. 10b. Finally, with the growth of load, the tenon was away from mortise slowly. In addition, the phenomenon was illustrated in the Fig. 10c and the Fig. 10d.

To further understand the stress distribution on joint, the mortise was studied in detail under the condition of Fig. 10a. It was obvious that the stress of different parts on mortise had exerted significant difference, the stress on curved surfaces were much larger than that on flat surfaces, Besides, the stress of flat surface was nearly zero. In addition, the distribution of stress was the same along with the length of mortise, which also confirmed that the third hypothesis described above was reasonable. Therefore, the distribution of stress on the whole curved surface could be represented by stress on its section as shown in Fig. 11. Furthermore, the stress of nodes along the arc section was extracted as shown in Fig. 12, it is obvious that the stress distribution of nodes on the section of the mortise were similar to a half oval, further illustrating that the mathematical model assembled above was reasonable.

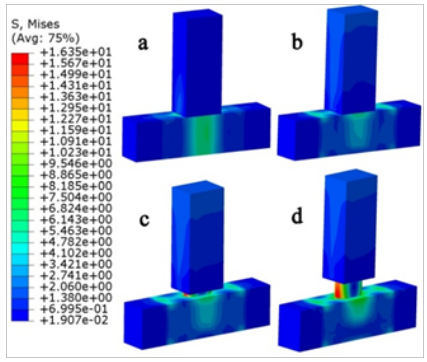

Fig.10: Stress distribution in different condition.

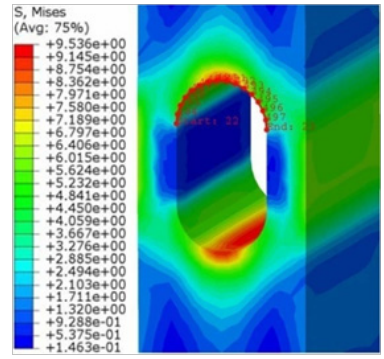

Fig.11: Stress distribution of mortise.

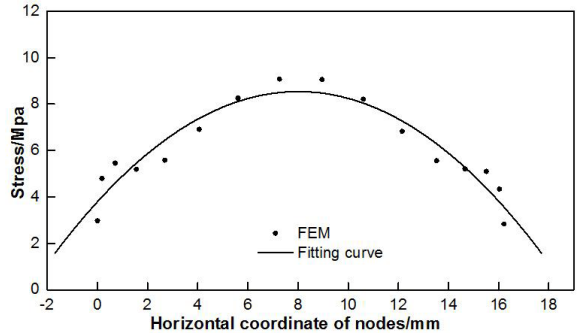

Fig. 12: Stress of nodes along the arc line on the cross section of mortise.

The reaction force of the reference point on the end of rail was 3126.27N, which was obtained through using numerical analysis based on the methods described above. According to the Newton's Third Law, the value of the reaction force is equal to the withdrawal force. In addition, the load displacement curve was able to be obtained by numerical analysis, shown in Fig. 13, and compared with the maximum and minimum withdrawal force of experiment.

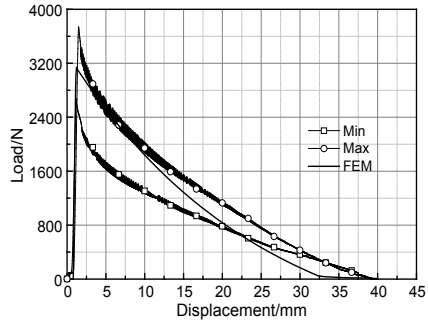

Fig. 13: Comparison of the FEM and experiment.

Tab. 2: The results and comparison of three methods.

Withdrawal force (N)				SD of FEM		SD of AM	
Min	Max	AM	FEM	Lower	Upper	Lower	Upper
2673.75	3736.88	2928.08	3126.27	16.9%	16.3%	9.5%	21.6%

Upper: refers to the percentage that the experimental maximum bigger than that of FEM.

Lower: refers to the percentage that the experimental minimum value smaller than that of FEM.

AM: refers to the result of Analytic Method.

SD: refers to Standard Deviation.

The Tab. 2 shows that the results of experiment, analytic method and numerical method respectively, and the deviations of them were figured out. It shows that the upper and lower deviation of the FEM is very close, but the upper deviation of the AM is twice bigger than lower deviation indicating that the FEM is more stable than AM. Besides, the consistency level between the numerical method and the experiment was nearly 83%, accounting for about 80% between

Analytic Method and experiment. They are all able to satisfy the need of engineering. However, due to the plasticity of material was not considered in the analytic method, the yield strength of radial direction is 9.831 N.mm-2 showed the mechanical properties of beech applied in the FEM. measured by the experiment, and the maximum contact stress of joint was 9.536 N.mm-2, as shown in the Fig. 11. Therefore, it was suggested that slight plastic deformation might be taken place, which is expected. Since at high interference values, the tube tends to deform plastically at an early stage, reducing the effective interference and thus the contact pressure and the friction force holding the two parts together (Hüyük et al. 2014).

CONCLUSIONS

To conclude, this study was carried out to investigate the methods of analyzing the withdrawal force of oval mortise and tenon joint based on numerical methods and analytic methods, and then verified the validity of them by conducting experiment. Finally, the characteristic and accuracy of them were compared and the final conclusions were as follows:

1) Different grains, pressure and contact area made no remarkable difference in friction coefficient on the basis of the processing type in this work.
2) The consistency level was 83 % and 80 % for the numerical method and the analytic method compared with experiment respectively. Besides, the result of FEM was more accurate than analytic method while the latter was simple and convenient.
3) The mathematical model established in the paper is suitable to evaluate the strength of joint, yet the plasticity is not taken into consideration.
4) The numerical method could forecast the stress distribution of oval tenon which is proved to be suitable to apply to furniture design as well as other wood-frame construction.

In conclusion, both the numerical method and the analytic method are applicable to analyze the withdrawal strength of joint in structure design of furniture and wood construction.

ACKNOWLEDGMENTS

This study was supported by National Forestry Public Welfare Industry Research Special with the project number: 2012047002021 and Jiangsu Provincial College of Science and Engineering PAPD.

REFERENCES

1. Çolakoğlu, M.H., Apay, A.C., 2012: Finite element analysis of wooden chair strength in free drop, International Journal of the Physical Sciences 7(7): 1105-1114.
2. Derikvand, M., Ebrahimi, G., 2014: Finite element analysis of stress and strain distributions in mortise and loose tenon furniture joints, Journal of Forestry Research 25(3): 677-681.
3. Desplanques, Y. 2015: Amontons-coulomb friction laws, A review of the original manuscript. SAE Int. J. Mater. Manf. 8(1): 98-103.
4. Divos, F., Tanaka, T., 1998: Determination of shear modulus on construction size timber, Wood Science and Technology 32(6): 393-402.

5. Douglas R., 2014: Withdrawal strength and bending yield strength of stainless steel nails, Journal of Structural Engineering 141(5): 1-7.
6. Dzincic, I., Skakic, D., 2012: Influence of type of fit on strength and deformation of oval tenon-mortise joint, Wood Research 57 (3): 469-477.
7. Eckelman, C. A., 2003: Textbook of product engineering and strength design of furniture. Purdue University Press, West Lafayette, Indiana.
8. Hu, W. G., 2015: Study of finite element analysis of node in solid wood structure furniture based on ANSYS, Furniture & Interior Design 46(11): 65-67.
9. Hüyük , H., Musica, M., 2014: Analysis of elastic-plastic interference-fit joints. 11th International Conference on Technology of Plasticity, ICTP 2014, Pp 19-24.
10. Kasal, A., Eckelman, C. A., Haviarova, E., Yalcin, I., 2015: Bending moment capacities of L-shaped mortise and tenon joints under compression and tension loadings, BioResources 10(4): 7009-7020.
11. Kasal, A., Smardzewski, J., Kuşkun, T., Ziya, Y., Erdil, Y. Z., 2016: Numerical analyses of various sizes of mortise and tenon furniture joints, BioResources1 1(3): 6836-6853.
12. Li, P., 2010:Mechanical analysis for typical mortising joints of wood product with finite element method, Wood Processing Machinery 25(02): 13-15.
13. Lv, Y.H., 2012: Application of finite element software ANSYS on strength analysis of fruitwood furniture, Journal of Northwest Forestry University 18 (06): 181-184.
14. Nuri, M., Karaman, A., Akinay, A., 2016: Finite element method application of wooden furniture, International Conference on Research in Education and Science.
15. Peng, X.R., 2012: Influence of lubricating and cooling mediums on frictional coefficient during wood cutting, China Wood Industry 26(5): 31-37.
16. Percin, O., 2016: Determination of screw withdrawal strength of heat treated and reinforced laminated veneer lumber, BioResources 11(1): 1729-1740.
17. Ringhofer, A., Grabner, M. Silva,C.V., Branco, J., 2014: The influence of moisture content variation on the withdrawal capacity of self -tapping screws, Holztechnologie 55(3): 33-40.
18. Shen M.X., Zheng J.P., Meng X.K., 2015: Fretting characteristics of fluorine rubber O-ring for reciprocating shaft seal, Journal of Mechanical Engineering 51(15): 39–45.
19. Smardzewski, J., 2015b: Furniture design, Springer, Heidelberg, Germany 377 pp.
20. Smardzewski, J., Papuga, T., 2004: Stress distribution in angle joints of skeleton Furniture, Electronic Journal of Polish Agricultural Universities. Wood Technology 7(1).
21. Shu, W., 2013: Study of joints of solid wood chair by finite element method, Master's Thesis. Central South University of Forestry and Technology, China.
22. Wang, Y., Lee, S., 2014: Design and analysis on interference fit in the hardwood dowel-glued joint by finite element method, Procedia Engineering 79: 166-172.
23. Xu, Z., Zhang, Ch., 2011: Dropping simulation analysis of the solid wood furniture based on ANSYS/LS-DYNA, Furniture & Interior Design 6(05): 13-15.
24. Yorur, H., Uysal, B., 2016: Simulating strength behaviors of corner joints of wood constructions by using finite element method, Drvna Industrija 67(2): 133-140.

Wen-Gang Hu, Hui-Yuan Guan*
Nanjing Forestry University
College of Furnishings and Industrial Design
210037 Nanjing
China
Phone: 150-7787-2795
Corresponding author: hwg@njfu.edu.cn